J. Mol. Model. **1995**, *1*, 176 - 187

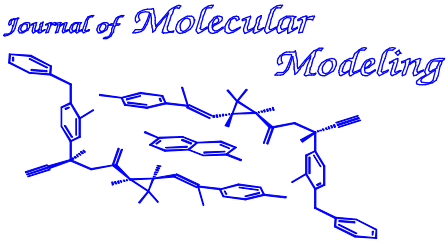

A Detailed Study of VESPA Electrostatic Potential-Derived Atomic Charges§

Bernd Beck, and Timothy Clark*

Computer-Chemie-Centrum, Institut für Organische Chemie, Friedrich-Alexander-Universität Erlangen-Nürnberg, Nägelsbachstraße 24, D-91052 Erlangen, Germany (clark@organik.uni-erlangen.de)

Robert C. Glen

Wellcome Research Laboratories, Langley Park, Beckenham, Kent, BR3 3BS, U.K.
Present address: Tripos Inc., 1699 South Hanley Road, St. Louis, MO 63144, USA.

§ We thank Graham Richards for acting as guest editor for this paper

Received: 5 October 1995 / Accepted: 20 October 1995

Abstract

VESPA, an improved semiempirical method for the calculation of electrostatic potential-derived atomic charges has been tested. It is shown that this approach is even less dependent upon molecular orientation than "high density" CHELPG *ab initio* ESP-derived charges. The conformational dependence of VESPA charges has been investigated for rotation around the C-N bond in formamide and 11 different conformers of glycerolphosphorylcholine. The results obtained are compared to the corresponding *ab initio* values. Finally, VESPA is used to calculate electrostatic potential-derived charges for bioorganic molecules. We discuss the abilities and the limitations of ESP charges in this area.

Keywords: Computational chemistry, potential-derived charges, orientational and conformational dependence

Introduction

It has been clear for some time that a representation of electrostatic interactions is important for the development of accurate molecular models. The best way to treat these interactions is still a matter of research and debate. However, point monopoles have gained acceptance because of their convenience, ease of application, low computational demands and intuitive feel [1-8]. Of the many different methods proposed for calculating these atomic point charges, a least squares fit to quantum mechanically derived electrostatic potentials has become a standard procedure [9-14].

We recently developed the VESPA approach to atomic point charges using semiempirical MO methods [15] in conjunction with a linear least squares fit procedure [16]. The points around the molecule were generated using a Marsili algorithm [17] with variable step size. All points within 1.4 times the van der Waals' radius of the molecule are eliminated. The maximum distance allowed is twice the vdW radius plus the step size.

The electrostatic potential at these points is then calculated using the NAO-PC model [18], which avoids the integral calculations of equation (1) and the disadvantages of the monopole approximation by representing each heavy atom by nine point charges (including the core charge).

* *To whom correspondence should be addressed*

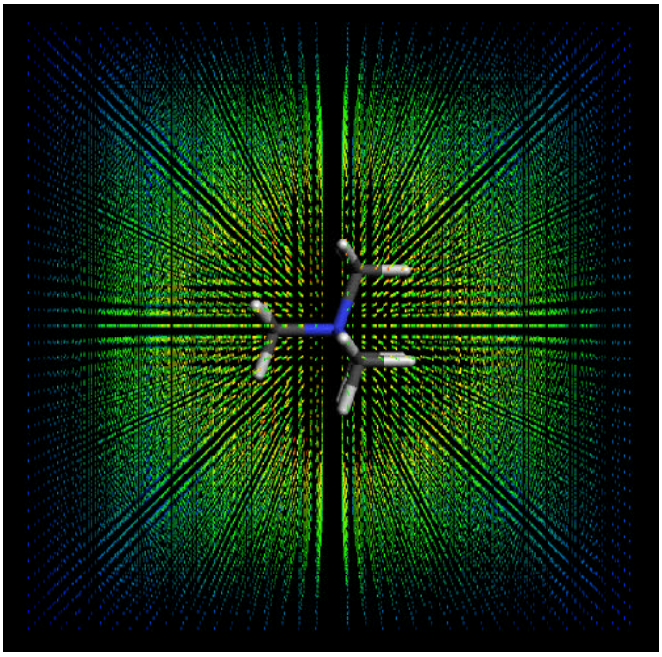

Figure 1. *Tetramethylammonium ion surrounded by a grid of points generated with VESPA. The color code is blue for the lowest electrostatic potential (34 kcal· mol^{-1}) and red for the highest (114 kcal· mol^{-1})*

The equation

$$V(r) = \sum_{\alpha} \frac{Z_\alpha}{|R_\alpha - r|} - \int \frac{\rho(r')dr'}{|r'-r|} \qquad (1)$$

becomes

$$V(\vec{r}) = \sum_{\alpha(\alpha \notin H)} \sum_{i=1}^{2norb+1} \frac{q_{i\alpha}}{|\vec{r}_{i\alpha} - \vec{r}|} + \sum_{\alpha(\alpha \in H)} \frac{q_\alpha}{|\vec{R}_\alpha - \vec{r}|} \qquad (2)$$

within the NAO-PC model, where V(r) is the potential at point r, $q_{i\alpha}$ the natural atomic orbital point charges (NAO-PCs) located at $r_{i\alpha}$ and q_α the charge of the hydrogen atoms located at R_α.

Overall this enables us to construct a very fast algorithm in which the most time-consuming step is the final linear least squares fit.

It was found that VESPA is able to reproduce MEP-derived atomic charges well relative to 6-31G* [19] *ab initio* calculations [15], especially for AM1 [20] and PM3 [21].

However, several key issues were not investigated in our initial paper. Firstly, we have not addressed the orientational dependence of our ESP charge technique. Breneman and Wiberg [14] found that the CHELP technique introduced by Chirlian and Francl [16] depended strongly on the orientation of a molecule in 3D space. Furthermore, they found that CHELP was unable to map the changes in atomic charges smoothly as the conformation changes. They introduced the modified CHELPG algorithm to mitigate these problems. Stouch and Williams analyzed the conformational dependency of ESP-derived monopoles for eleven different conformers of glycerolphosphorylcholine (GPC) [22] in order to use them for subsequent investigations of dynamic properties.

In this paper we investigate the orientational and conformational dependence of VESPA charges and compare the results to *ab initio* results as far as possible. The second part of the paper deals with the ability of VESPA to calculate ESP atomic charges for bioorganic systems (polypeptides) between 140 and 300 atoms.

Computational methods

All structures used were optimized using the semiempirical program package VAMP5.5[23]. For the eleven different GPC conformers, the zwitterionic headgroup of many biological important lipids, we used the PM3 Hamiltonian [21]. All other calculations used AM1 [20]. In order to be able to compare our results to *ab initio* values we optimized the structures corresponding to those used by Breneman and Wiberg (formamide) and Stouch and Williams (GPC). The ESP-derived monopoles were calculated with VESPA using a high density grid (0.2 - 0.3 Å step size) for the charge-fitting procedure. All calculations used an Indigo^2 (R4400, 200MHz) workstation or a Power Challenge (R8000, 75 Mhz).

Results and discussion

Orientational dependence

In the first part of this study we calculate the electrostatic potential-derived monopoles for the planar minimum (**1**) and the *syn* rotational transition state(**2**) of formamide orientated in various

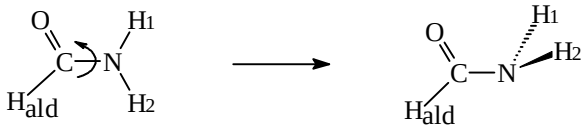

1 **2**

directions in 3D space. The results obtained are compared to those reported using the high density CHELPG (6-31G**) method [14]. The values for **2** are shown in Table 1 and those for **1** in Table 2. In each of these tables the structures labeled "normal" refer to the orientation in which the C-N bond is colinear with the *x*-axis and the heavy atoms are in

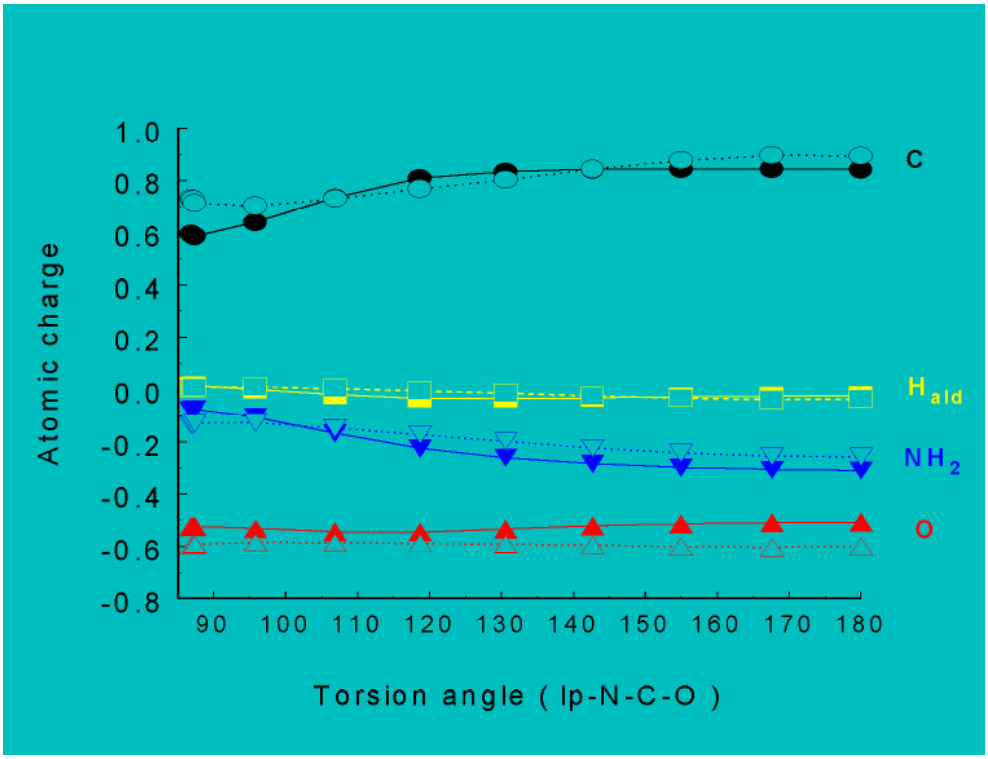

Figure 2. *Atomic charge variations along the C-N rotational pathway for formamide*

the *xz* plane. The other orientations were produced by rotating the indicated amount about the specified axis.

The average nitrogen charge was calculated with VESPA to be -1.1362 (-1.0650 using CHELPG) , while the carbon and oxygen charges were calculated to be 0.8412 (0.9482) and-0.5076 (-0.6164), respectively. The aldehyde hydrogen is negative in both cases. It is remarkable that the atomic charges of the symmetry-related hydrogens H_1 and H_2 differ only between 0.0001 and 0.0008 for the different orientations. For the planar formamide the difference between the VESPA charges and the CHELPG charges are larger than for the transition state, especially for the N and C atoms.

The average nitrogen monopole is -0.6405 (-0.9896) and for the carbon atom we obtained 0.5582 (0.7134). The oxygen charges are similar to the transition structure. In the case of the aldehyde hydrogen VESPA gives a slightly negative charge, while CHELPG still calculates a small positive charge for this atom.

The standard deviations of the charges in the different orientations obtained with VESPA are equal or even less than those of the CHELPG charges. Especially for the planar formamide all standard deviations derived from our algorithm are smaller than the corresponding CHELPG values.

Conformational dependence

Formamide

We have chosen formamide as a worst possible case for semiempirical MO-methods because of the known [21] problems of AM1 and PM3 with the geometry and the rotation barrier of amide C-N bonds. The atomic charge variations for the calculations along the C-N rotational pathway are shown in Table 3. The column marked „ lp-N-C-O“ indicates the dihedral angle between the „lone pair“ vector and the carbonyl group.

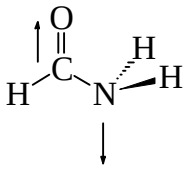

The first row of the table gives the structure is in its planar form. As the rotation progresses the dihedral angle increases to 180°. Figure 2 depicts the changes of the atomic charges along the pathway. The heavy line indicates the high density VESPA charges, and the lighter line (empty symbols) those from CHELPG .

Although the overall changes in the ESP atomic charges of the NH_2 group are larger for VESPA, both methods give similar qualitative results (blue curves in Figure 2). As expected from simple electrostatic potential considerations, the total charge on the amino group is less negative in the planar conformation than in the transition structure. The changes in the potential-derived carbonyl carbon charge are shown as black curves in Figure 2. Again the trends are similar for the two methods. It is also significant that the change in the C charge is nearly equal and opposite to the amino group variation.

The VESPA carbonyl oxygen charge changes only marginally between the starting and the final points of the pathway (red curves in Figure 2). The two calculational approaches show opposite trends but the changes are only of the order of 10^{-2} e^-. Similarly, for the aldehyde hydrogen the changes are small and the trends given by the two methods agree resonable well.

The results presented suggest that the amino nitrogen in the planar form is less negative than in the *syn* rotational transition state. This is in good agreement with some of the established properties of planar and rotationally deformed amides [24]. The lack of change of the carbonyl oxygen monopole, however, is contrary to the widely accepted explanation for amide resonance,but agrees with the explanation of amide stabilization by Wiberg [25] and NRT investigations of Weinhold [26].

GPC

As a second test of the conformational dependence of VESPA ESP atomic charges, we calculated the monpoles for eleven different conformers of glycerolphosphorylcholine (GPC), similar to those published by Stouch and Williams [22]. The values of the torsion angles which were held fixed during the PM3 optimisation are given in Table 4. The atom-numbering is shown in Figure 3.

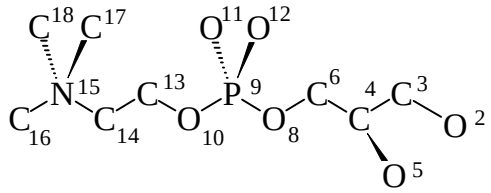

Figure 3. *Structure and atomic numbering scheme for GPC Hydrogen atoms are not shown; numbering corresponds to the number of the atom to which they are attached, e. g., H61 is hydrogen atom 1 attached to carbon atom 6*

The calculated VESPA atomic charges for the individual conformations are shown in Table 5, the corresponding charge statistics (univariant statistic for each atom), together with the *ab initio* values for the standard deviations and the range are given in table 6.

Statistics for the charges of individual atoms (Table 6) show that the range of the charge for a particular atom varies greatly. While the charges vary by less than 0.2 electron units (eu) for many atoms, the range can be up to 0.53, as seen for P9. As noted before [15] the charges for those atoms on the "outside" of the molecule (closest to the electrostatic potential) tend to vary the least while those for atoms on the "inside" vary most (e.g. N15 and P9). The charges for hydrogens typically vary the least, with a standard deviation of about 0.06.

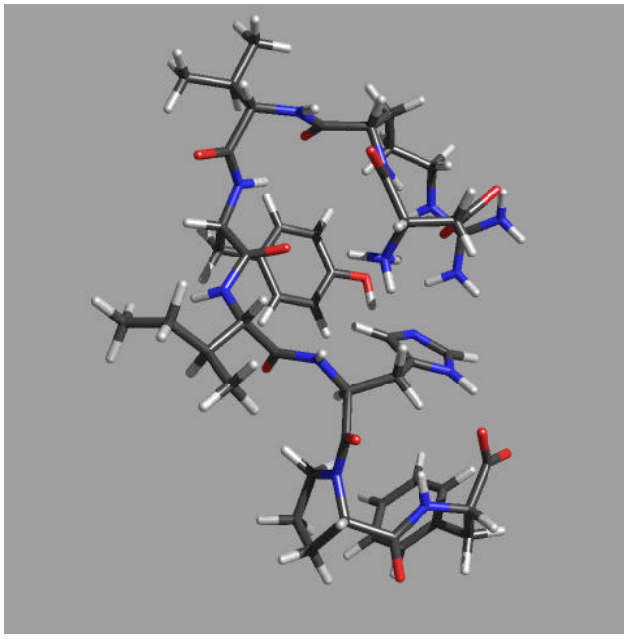

Figure 6. *Angiotensin II*

Compared to the *ab initio* (6-31G*) values presented by Stouch and Williams, nearly all range values and standard deviations obtained with the high density VESPA method are lower.

ESP- derived atomic charges for bioorganic molecules

Finally, we have investigated the ability of VESPA to calculate electrostatic potential-derived atomic charges for bioorganic molecules between 140 and 300 atoms. We have used the octapeptide angiotensin II (146 atoms) shown in Figure 4 as the first test molecule.

The resulting atomic charges are compared to those assigned by the AMBER [27] force field. The values for the heavy atoms are shown in Figure 7.

In most parts of the molecule there is a good agreement between the two methods. The strongest deviations occur where interactions like hydrogen bonds occur. VESPA charges take these interactions into account, whereas AMBER assigns the charges according to the different residue types. Therefore the VESPA-derived atomic charges are more reliable than the AMBER monopoles in such parts of the molecule. Consider, for example, the interaction between one oxygen of the CO_2^- group of Phe8 with the NH_2 group in the imidazole ring of His6.

Other examples for such important interactions are between the oxygen in Tyr4 and an amino group of Arg2 or the interaction of the CO_2^- group in asparagine with the NH_3^+ group in the same residue. There are a many such interac-

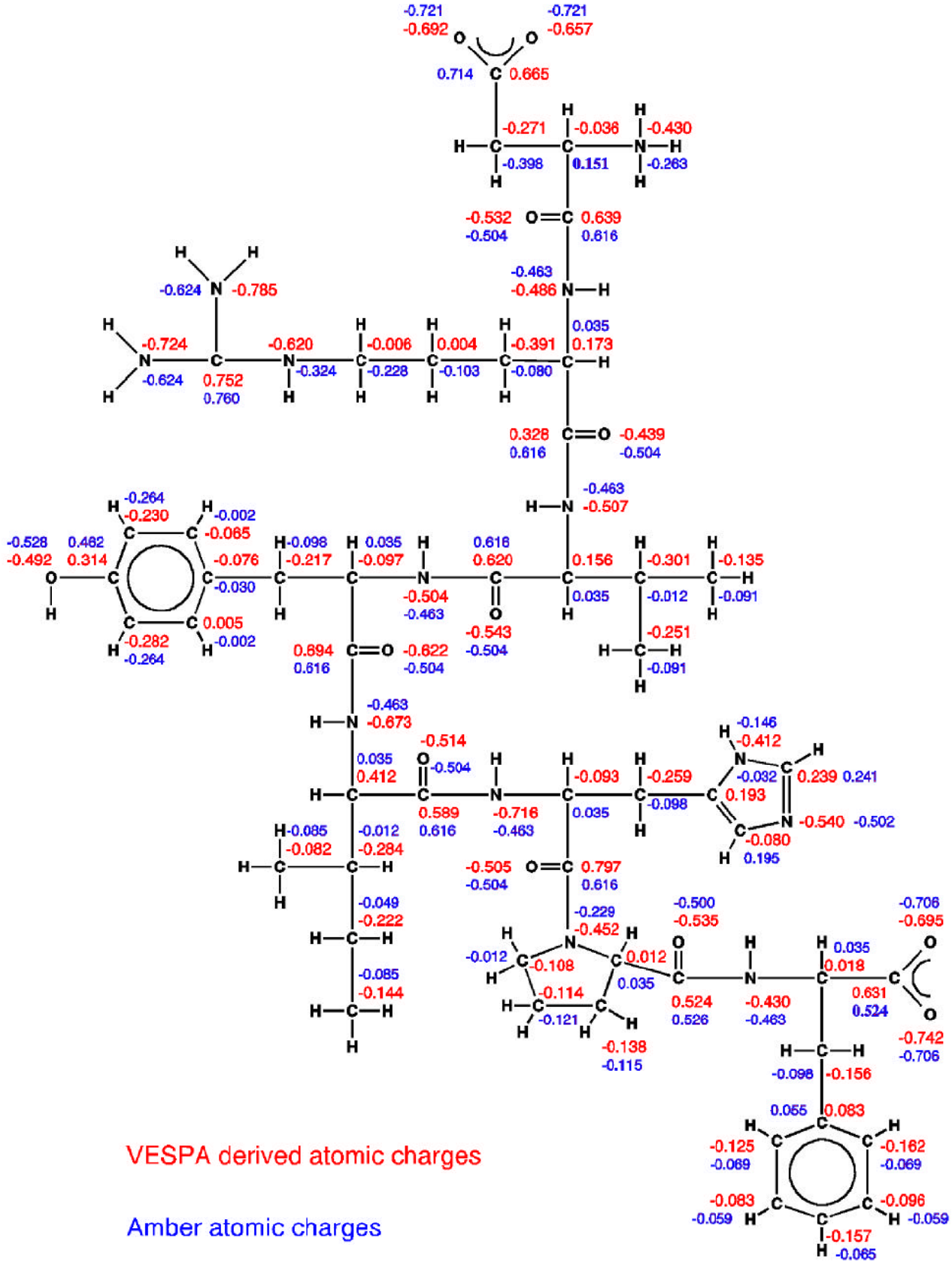

Figure 7. *Angiotensin II, VESPA (red) and Amber (blue) atomic charges*

tions which influence the individual atomic charges. Therefore, the charges change with the conformation of the molecule (see above). The VESPA calculations described above used a step size of 0.3 Å. This results in the generation of 291,647 grid points for the charge-fitting procedure. The entire calculation requires 1667 seconds on a Power Challenge.

Encouraged by the results above, we used our approach to calculate the electrostatic potential- derived atomic charges for an α-helix polypeptide containing 28 alanine residues (292 atoms).

The charges obtained range between 491530.34 and -653600.60. These values have no chemical relevance. The reason is shown in Figure 8. The helix structure produces a cavity in which no or only a few grid points for the charge fitting procedure are generated.. Therefore, the electrostatic potential around the atoms inside the helix is not well defined and, thus, their ESP-derived atomic charges.

Conclusions

We have shown that the VESPA approach to determining electrostatic potential-derived atomic charges using semiempirical techniques is essentially orientationally invariant. Conformational variation gives smooth and reasonable changes in both the molecular electrostatic potential and the charges derived from it. The high density VESPA technique allows conformational studies, as shown by the analysis of the formamide molecule during the C-N bond rotation and the results for the eleven conformers of GPC. The monopoles obtained are in good agreement with *ab initio* 6-31G* and 6-31G** calculations. VESPA thus gives comparable or better results than the *ab initio* methods in a fraction of their CPU times.

Since this method is so effective at generating monopoles that reproduce the electrostatic potential of a molecule, it is possible to use VESPA for larger bioorganic systems. In this case, however, there is a critical relationship between the structure of the molecule and the quality of the results. This is a general disadvantage of all methods that use grid points in a defined distance around a molecule.

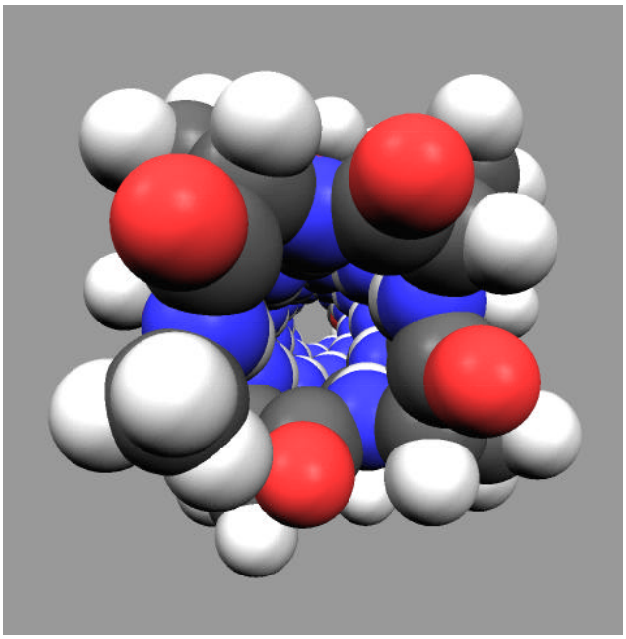

Figure 8. *Cavity formed by the* $(Ala)_{28}$ *α-helix*

Acknowledgement: B. B. thanks the Wellcome Foundation Ltd., Beckenham,Kent, U.K. for financial support

References

1. Mulliken, R. S. *J. Chem. Phys.*, **1955**, *23*, 1833.
2. Del Re, G. *J. Chem. Soc.*, **1958**, 4031.
3. Abraham, R. J. and Hudson, B. *J. Comp. Chem.*, **1985**, *6*, 173.
4. Abraham, R. J. and Smith, P. E. *J. Comp. Chem.*, **1987**, *9*, 288.
5. Mortier, W. J.; Gosh, S. K. and Shankar, S. *J. Am. Chem. Soc.*, **1986**, *108*, 4315.
6. Williams, D. E. *J. Comp. Chem.*, **1988**, *9*, 745.
7. Mullay, J. *J. Comp. Chem.*, **1988**, *9*, 309.
8. Price, S. L.; Harrison, R. J. and Guest, M. F. *J. Comp. Chem.*, **1989**, *10*, 552.
9. Ferenczy, G. G.; Reynolds, C. A. and Richards, W. G. *J. Comp. Chem.*, **1990**, *11*, 159.
10. Orozco, M. and Lugue, F. J. *J. Comp. Chem.*, **1990**, *11*, 909.
11. Cox, S. R. and Williams, D. E. *J. Comp. Chem.*, **1981**, *2*, 304.
12. Besler, B. H.; Merz K. M. and Kollman, P. A. *J. Comp. Chem.*, **1990**, *11*, 431.
13. Merz K. M. *J. Comp. Chem.*, **1992**, *13*, 749.
14. Breneman, C. M. and Wiberg, K. B. *J. Comp. Chem.*, **1990**, *11*, 361.
15. Beck, B., Glen, R. C. and Clark, T., *J. Comp. Chem.*, submitted.
16. Chirlian, L. E. and Francl, M. M. *J. Comp. Chem.*, **1987**, *8*, 894.
17. a) Heiden, W.; Goetze, T. and Brickmann, J. *J. Comp. Chem.*,**1993**, *14*, 246.
    b) Lorensen, W.; Cline, H. *Comp. Graph.*, **1987**, *21*, 163.
18. a) Rauhut, G. and Clark, T., *J. Comp. Chem.*, **1993**, *14*, 503.
    b) Beck, B., Rauhut, G. and Clark, T., *J. Comp. Chem.*,**1994**, *15*, 1064.
19. Hehre W. J.; Radom, L.; Schleyer, P.v.R. and Pople, J. A. *Ab Initio Molecular Orbital Theory*, John Wiley & Sons, New York, **1986**.
20. Dewar, M. J. S; Zoebisch, E. G.; Hersley, E. F. and Stewart, J. J. P. *J. Am. Chem. Soc.*, **1985**, *107*, 3902.
21. Stewart, J. J. P. *J. Comp. Chem.*, **1989**, *10*, 209.

22. Stouch, T. R. and Williams, D. E. *J. Comp. Chem.*, **1992**, *13*, 622.
23. Rauhut, G.; Alex, A.; Chandrasekhar, J.; Steinke, T.; Sauer, W.; Beck, B. and Clark, T. **VAMP V5.5**, Oxford Molecular Ltd., Magdalen Centre, Oxford Science Park, Sandford-on-Thames, Oxford, OX4 4GA, England.
24. Greenberg, A. in Structure and Reactivity Liebman, J. F. and Greenberg, A., Eds, VCH Publishers: Deerfield Beach, FL, **1987**, Chapter 4.
25. Wiberg, K. B. and Laidig, K. E. *J. Am. Chem. Soc.*, **1987**, *109*, 5935.
26. Weinhold, F. private communications.
27. Pearlman, D. A.; Case, D. A. ; Caldwell, J. W.; Ross, W. S.; Cheatham III, T. E.; Ferguson, D. M.; Seibel, G. L.; Singh, U. C.; Weiner, P. K.; and Kollman P. A. **AMBER** 4.1, University of California, San Francisco, **1995**. (available from Oxford Molecular Ltd., Magdalen Centre, Oxford Science Park, Sandford-on-Thames, Oxford, OX4 4GA, England.

Table 1. *VESPA (bold) and CHELPG [a] electronic charges of formamide* syn *rotational transition state*

Orientation	N	C	O	H(ald)	H1	H2	Dipole [b]	Points
Normal	**-1.1392**	**0.8423**	**-0.5073**	**-0.2340**	**0.4134**	**0.4142**	**1.237**	**94532**
	-1.0650	0.9482	-0.6164	-0.0628	0.3980	0.3980	1.626	6007
30°(x)	**-1.1365**	**0.8411**	**-0.5074**	**-0.2302**	**0.4128**	**0.4129**	**1.230**	**89708**
	-1.0626	0.9429	-0.6147	-0.0615	0.3978	0.3980	1.631	5983
30°(y)	**-1.1333**	**0.8400**	**-0.5077**	**-0.2292**	**0.4119**	**0.4120**	**1.235**	**91152**
	-1.0615	0.9479	-0.6168	-0.0636	0.3970	0.3970	1.637	5978
30°(z)	**-1.1366**	**0.8407**	**-0.5075**	**-0.2275**	**0.4127**	**0.4135**	**1.232**	**94528**
	-1.0638	0.9439	-0.6153	-0.0610	0.3979	0.3983	1.629	5966
45°(x)	**-1.1366**	**0.8423**	**-0.5077**	**-0.2338**	**0.4126**	**0.4127**	**1.230**	**91145**
	-1.0614	0.9397	-0.6133	-0.0602	0.3979	0.3974	1.628	6000
45°(y)	**-1.1346**	**0.8411**	**-0.5078**	**-0.2347**	**0.4124**	**0.4124**	**1.235**	**94561**
	-1.0625	0.9431	-0.6148	-0.0614	0.3978	0.3978	1.631	5982
45°(z)	**-1.1367**	**0.8412**	**-0.5078**	**-0.2291**	**0.4131**	**0.4132**	**1.232**	**94734**
	-1.0609	0.9418	-0.6143	-0.0610	0.3972	0.3972	1.630	5980
Average	**-1.1362**	**0.8412**	**-0.5076**	**-0.2310**	**0.4127**	**0.4130**		
	-1.0625	0.9439	-0.6151	-0.0616	0.3977	0.3977		
Std. Dev.	**0.0019**	**0.0008**	**0.0002**	**0.0003**	**0.0005**	**0.0007**		
	0.0015	0.0031	0.0012	0.0012	0.0004	0.0005		

[a] Taken from reference [14]
[b] Dipole moment (Debye) calculated from VESPA (CHELPG) charges; The Hamiltonian based AM1 dipole moment is 1.217 D, that of 6-31G 1.573 D*

Table 2. *VESPA (bold) and CHELPG [a] electronic charges of planar formamide*

Orientation	N	C	O	H(ald)	H1	H2	Dipole [b]	Points
Normal	**-0.6405**	**0.5582**	**-0.5183**	**0.0235**	**0.3002**	**0.2768**	**3.681**	**79197**
	-0.9896	0.7934	-0.6191	-0.0247	0.4357	0.4043	4.090	5940
30°(x)	**-0.6412**	**0.5605**	**-0.5190**	**0.0227**	**0.3002**	**0.2768**	**3.681**	**82382**
	-0.9926	0.8032	-0.6226	-0.0282	0.4356	0.4047	4.091	5977
30°(y)	**-0.6399**	**0.5582**	**-0.5186**	**0.0235**	**0.3001**	**0.2767**	**3.686**	**86207**
	-0.9879	0.7900	-0.6184	-0.0229	0.4354	0.4038	4.087	5939
30°(z)	**-0.6408**	**0.5593**	**-0.5186**	**0.0230**	**0.3003**	**0.2768**	**3.680**	**86949**
	-0.9962	0.8004	-0.6213	-0.0265	0.4375	0.4061	4.110	5973
45°(x)	**-0.6424**	**0.5619**	**-0.5195**	**0.0224**	**0.3005**	**0.2771**	**3.682**	**82577**
	-0.9919	0.7964	-0.6205	-0.0251	0.4363	0.4048	4.092	5959
45°(y)	**-0.6405**	**0.5583**	**-0.5185**	**0.0234**	**0.3004**	**0.2769**	**3.682**	**86223**
	-0.9891	0.7909	-0.6189	-0.0229	0.4361	0.4039	4.092	5941
45°(z)	**-0.6416**	**0.5605**	**-0.5190**	**0.0226**	**0.3006**	**0.2769**	**3.682**	**85156**
	-0.9964	0.8045	-0.6225	-0.0284	0.4369	0.4059	4.089	5966
Average	**-0.6410**	**0.5596**	**-0.5188**	**0.0230**	**0.3003**	**0.2769**		
	-0.9920	0.7970	-0.6205	-0.0255	0.4362	0.4048		
Std. Dev.	**0.0034**	**0.0059**	**0.0017**	**0.0023**	**0.0008**	**0.0009**		
	0.0008	0.0014	0.0004	0.0005	0.0002	0.0001		

[a] Taken from reference [14]

[b] Dipole moment (Debye) calculated from VESPA (CHELPG) charges; The Hamiltonian based AM1 dipole moment is 3.698 D, that of 6-31G 4.095 D*

Table 3. *VESPA (bold) and CHELPG [a] electronic charges of form-amide during rotation from planar to* syn *rotational transition state*

Lp-N-C-O	N	C	O	H(ald)	H1	H2
86.8°	**-0.6820**	**0.5942**	**-0.5253**	**0.0123**	**0.2908**	**0.3100**
	-0.9843	0.7277	-0.5970	0.0035	0.4414	0.4087
87.1°	**-0.6749**	**0.5889**	**-0.5243**	**0.0138**	**0.2884**	**0.3081**
	-0.9833	0.7267	-0.5970	0.0035	0.4414	0.4087
87.3°	**-0.6709**	**0.5859**	**-0.5238**	**0.0147**	**0.2870**	**0.3071**
	-0.9623	0.7117	-0.5920	0.0074	0.4344	0.4007
95.8°	**-0.7400**	**0.6386**	**-0.5330**	**-0.0006**	**0.3107**	**0.3243**
	-0.9293	0.7007	-0.5840	0.0095	0.4154	0.3877
106.9°	**-0.8908**	**0.7327**	**-0.5443**	**-0.0215**	**0.3611**	**0.3628**
	-0.9463	0.7287	-0.5850	0.0035	0.4134	0.3857
118.7°	**-1.0334**	**0.8077**	**-0.5457**	**-0.0352**	**0.4071**	**0.3995**
	-0.9693	0.7667	-0.5890	-0.0055	0.4104	0.3867
130.6°	**-1.0960**	**0.8323**	**-0.5347**	**-0.0356**	**0.4230**	**0.4110**
	-0.9953	0.8027	-0.5910	-0.0135	0.4084	0.3887
142.7°	**-1.1205**	**0.8403**	**-0.5230**	**-0.0322**	**0.4238**	**0.4116**
	-1.0243	0.8427	-0.5950	-0.0245	0.4074	0.3927
155.0°	**-1.1297**	**0.8428**	**-0.5148**	**-0.0283**	**0.4197**	**0.4104**
	-1.0483	0.8757	-0.6010	-0.0325	0.4084	0.3967
167.6°	**-1.1342**	**0.8428**	**-0.5096**	**-0.0250**	**0.4153**	**0.4108**
	-1.0613	0.8947	-0.6020	-0.0385	0.4064	0.3997
180.0°	**-1.1355**	**0.8409**	**-0.5074**	**-0.0229**	**0.4126**	**0.4123**
	-1.0673	0.8937	-0.5990	-0.0365	0.4044	0.4047

[a] Taken from reference [14]

Table 4. *Torsion angles of the GPC conformers [a]*

Atoms	Conformer number										
	k1	**k2**	**k3**	**k4**	**k5**	**k6**	**k7**	**k8**	**k9**	**k10**	**k11**
H21 O2 C3 C4	340.0	141.2	141.2	141.2	141.2	141.2	141.2	175.8	196.9	68.5	217.1
O2 C3 C4 O5	180.4	170.4	170.4	170.4	60.3	60.3	170.4	57.7	69.0	64.8	67.3
O2 C3 C4 C6	297.1	290.5	290.5	290.5	180.4	180.4	290.5	176.4	188.5	186.5	187.0
C3 C4 O5 H51	290.2	282.9	282.9	282.9	282.9	282.9	282.9	42.7	77.3	177.4	358.3
C3 C4 C6 O8	172.3	297.0	297.0	297.0	179.9	179.9	287.0	173.5	183.2	59.1	57.4
C4 C6 O8 P9	164.6	188.4	188.4	188.4	179.0	179.2	188.4	172.3	277.4	74.9	175.5
C4 O8 P9 O10	288.6	63.8	63.8	63.8	179.6	21.5	63.8	306.9	173.2	291.3	55.3
C4 O8 P9 O11	40.5	313.0	313.0	313.0	68.8	270.7	313.0	190.7	58.1	176.9	297.3
C4 O8 P9 O12	173.8	178.7	178.7	178.7	294.5	136.4	178.7	60.3	289.3	46.5	169.7
O8 P9 O10 C13	301.1	159.9	65.4	65.4	177.8	177.4	65.4	290.3	300.0	173.7	222.4
P9 O10 C13 C14	221.9	139.8	123.9	235.9	179.6	144.8	139.8	154.6	84.1	267.1	281.0
O10 C13 C14 N15	72.6	284.6	284.6	284.6	180.6	57.6	284.6	167.7	63.0	176.9	292.1
C13 C14 N15 C16	292.0	68.0	68.0	68.0	68.0	68.0	127.9	292.3	294.9	299.8	305.3
C13 C14 N15 C17	56.8	306.1	306.1	306.1	306.1	306.1	6.0	54.8	56.8	62.2	186.2
C13 C14 N15 C18	174.0	184.3	184.3	184.3	184.3	184.3	244.2	173.9	175.9	181.1	67.1

[a] Taken from reference [22]

Table 5. *VESPA charges for 11 conformers of GPC*

	conformer number										
Atom	**k1**	**k2**	**k3**	**k4**	**k5**	**k6**	**k7**	**k8**	**k9**	**k10**	**k11**
H21	0.3165	0.3308	0.3344	0.3326	0.3158	0.3120	0.3362	0.3131	0.2988	0.2959	0.3043
O2	-0.4991	-0.5098	-0.5017	-0.5140	-0.4966	-0.4814	-0.5062	-0.4809	-0.4656	-0.4536	-0.4838
C3	0.0084	0.1180	0.0895	0.1617	0.0910	0.0616	0.0742	0.0728	0.1430	0.0366	0.1121
C4	0.0882	-0.0551	0.0111	-0.0501	0.0040	0.0355	0.0334	0.0184	-0.0992	-0.2102	-0.0382
O5	-0.4797	-0.4562	-0.4634	-0.4693	-0.4292	-0.4283	-0.4617	-0.4568	-0.4522	-0.4160	-0.4935
C6	-0.0449	0.2385	0.0832	0.1422	0.0286	0.1614	0.0987	0.2041	0.0163	0.2368	0.2647
H51	0.2947	0.3101	0.3022	0.3027	0.2997	0.3047	0.2991	0.2854	0.2921	0.2936	0.3146
O8	-0.7808	-0.7252	-0.6643	-0.7062	-0.6697	-0.7208	-0.6978	-0.7379	-0.6900	-0.7386	-0.7379
P9	2.7690	2.3887	2.3133	2.3015	2.3297	2.3271	2.3627	2.2826	2.3137	2.2923	2.2419
O10	-0.8405	-0.7413	-0.7457	-0.7895	-0.8109	-0.7926	-0.7527	-0.7429	-0.7539	-0.7275	-0.7438
O11	-1.1900	-1.0575	-0.9750	-0.9857	-1.0212	-0.9906	-0.9881	-0.9918	-0.9830	-0.9757	-0.9930
O12	-1.2353	-0.9926	-1.0550	-0.9783	-1.0148	-0.9781	-1.0391	-0.9702	-0.9753	-1.0449	-0.9842
C13	0.1928	0.0914	0.1830	0.3533	0.4277	0.2277	0.1617	0.3323	0.3521	0.2123	0.2350
C14	-0.0794	-0.1149	-0.1743	-0.2631	-0.2160	-0.1818	-0.0623	-0.2746	-0.5502	-0.1783	-0.2237
N15	-0.0872	0.3346	0.3256	0.2465	0.2550	0.4358	0.2653	0.2038	0.3464	0.1933	0.2763
C16	-0.1981	-0.4560	-0.4539	-0.2685	-0.2663	-0.3212	-0.2463	-0.2442	-0.2611	-0.1555	-0.2678
C17	-0.2327	-0.2740	-0.2752	-0.2949	-0.2148	-0.4222	-0.2937	-0.0770	-0.2768	-0.2006	-0.3326
C18	-0.2207	-0.3633	-0.3496	-0.3274	-0.3273	-0.3911	-0.3033	-0.2868	-0.3117	-0.2547	-0.3038
H31	0.0623	0.0315	0.0346	0.0207	0.0572	0.0521	0.0370	0.0283	0.0251	0.0973	0.0325
H32	0.0992	0.0631	0.0580	0.0505	0.0320	0.0327	0.0660	0.0460	0.0299	0.0851	0.0613
H41	0.0953	0.0815	0.0811	0.0751	0.0922	0.0820	0.0742	0.1230	0.1705	0.1536	0.1163
H61	0.0960	-0.0005	0.0402	0.0329	0.0587	0.0099	0.0359	-0.0333	0.0301	0.0050	0.0093
H62	0.1172	0.0021	0.0471	-0.0167	0.0400	-0.0439	0.0315	-0.0101	0.0638	0.0408	-0.0231
H131	0.0690	0.0375	0.0026	-0.0213	-0.0610	0.0346	-0.0142	-0.0271	0.0106	0.0099	0.0075
H132	0.0175	0.0618	0.0434	-0.0139	-0.0511	-0.0174	0.0448	-0.0286	-0.0150	0.0135	0.0282
H141	0.1058	0.1381	0.1446	0.2310	0.1379	0.0936	0.1009	0.1574	0.1767	0.1132	0.1814
H142	0.1542	0.0911	0.1028	0.1161	0.1372	0.1398	0.0747	0.1497	0.3182	0.1501	0.1123
H161	0.1448	0.2444	0.2690	0.1882	0.1680	0.1846	0.1696	0.1374	0.1217	0.1271	0.1208
H162	0.1965	0.1555	0.1652	0.1264	0.1376	0.1262	0.1065	0.1650	0.1587	0.1423	0.1695
H163	0.1369	0.1611	0.1622	0.1256	0.1262	0.1378	0.1049	0.1190	0.1293	0.0936	0.1303
H171	0.1381	0.1444	0.1457	0.1421	0.1165	0.1319	0.1163	0.0784	0.1240	0.1103	0.1256
H172	0.2189	0.1280	0.1282	0.1368	0.1315	0.1485	0.1120	0.1253	0.1808	0.1467	0.1697
H173	0.1400	0.1606	0.1666	0.1786	0.1411	0.2780	0.2450	0.1015	0.1199	0.1086	0.1455
H181	0.1385	0.1456	0.1450	0.1595	0.1558	0.1519	0.1287	0.1385	0.1437	0.1304	0.1812
H182	0.1431	0.1433	0.1400	0.1464	0.1519	0.1624	0.1553	0.1475	0.1523	0.1568	0.1486
H183	0.1445	0.1449	0.1396	0.1288	0.1434	0.1378	0.1307	0.1328	0.1160	0.1105	0.1361

Table 6. *Charge statistics*

Atom	Minimum	Maximum	Mean	ab initio Mean [a]	Std. Dev.	ab initio Std.Dev. [a]	Range	ab initio Range [a]
H21	0.2959	0.3362	0.3173	0.493	0.0144	0.028	0.040	0.084
O2	-0.5140	-0.4536	-0.4902	-0.874	0.0190	0.061	0.060	0.162
C3	0.0084	0.1617	0.0881	0.383	0.0448	0.138	0.153	0.453
C4	-0.2102	0.0882	-0.0238	0.371	0.0809	0.171	0.298	0.647
O5	-0.4935	-0.4160	-0.4551	-0.843	0.0231	0.070	0.077	0.235
C6	-0.0449	0.2647	0.1300	0.258	0.1024	0.258	0.310	0.970
H51	0.2854	0.3146	0.2999	0.477	0.0083	0.031	0.029	0.095
O8	-0.7808	-0.6643	-0.7154	-0.607	0.0342	0.137	0.117	0.485
P9	2.2419	2.7690	2.3566	-1.890	0.1422	0.142	0.527	0.498
O10	-0.8405	-0.7275	-0.7674	-0.776	0.0356	0.118	0.113	0.394
O11	-1.1900	-0.9750	-1.0138	-1.006	0.0631	0.045	0.215	0.127
O12	-1.2353	-0.9702	-1.0244	-0.983	0.0764	0.031	0.265	0.167
C13	0.0914	0.4277	0.2517	0.504	0.1011	0.350	0.336	1.317
C14	-0.5502	-0.0623	-0.2108	-0.465	0.1319	0.231	0.488	0.742
N15	-0.0872	0.4358	0.2541	0.098	0.1329	0.125	0.523	0.380
C16	-0.4560	-0.1555	-0.2854	-0.507	0.0938	0.091	0.301	0.285
C17	-0.4222	-0.0770	-0.2631	-0.532	0.0862	0.156	0.345	0.496
C18	-0.3911	-0.2207	-0.3127	-0.561	0.0481	0.057	0.170	0.179
H31	0.0207	0.0973	0.0435	-0.006	0.0223	0.029	0.077	0.097
H32	0.0299	0.0992	0.0567	-0.008	0.0219	0.042	0.069	0.117
H41	0.0742	0.1705	0.1041	0.059	0.0329	0.036	0.096	0.108
H61	-0.0333	0.0960	0.0258	0.110	0.0340	0.059	0.129	0.216
H62	-0.0439	0.1172	0.0226	0.094	0.0464	0.072	0.161	0.314
H131	-0.0610	0.0690	0.0044	0.017	0.0354	0.099	0.130	0.368
H132	-0.0511	0.0618	0.0076	0.029	0.0354	0.102	0.113	0.338
H141	0.0936	0.2310	0.1437	0.244	0.0413	0.061	0.137	0.159
H142	0.0747	0.3182	0.1406	0.216	0.0645	0.086	0.244	0.308
H161	0.1208	0.2690	0.1705	0.263	0.0491	0.043	0.148	0.154
H162	0.1065	0.1965	0.1499	0.238	0.0252	0.029	0.090	0.092
H163	0.0936	0.1622	0.1297	0.227	0.0205	0.031	0.069	0.102
H171	0.0784	0.1457	0.1248	0.250	0.0196	0.054	0.067	0.182
H172	0.1120	0.2189	0.1479	0.268	0.0309	0.036	0.107	0.175
H173	0.1015	0.2780	0.1623	0.230	0.0549	0.059	0.177	0.103
H181	0.1287	0.1812	0.1472	0.246	0.0148	0.026	0.053	0.070
H182	0.1400	0.1624	0.1498	0.250	0.0067	0.023	0.022	0.067
H183	0.1105	0.1449	0.1332	0.251	0.0113	0.024	0.034	0.080

[a] Taken from reference [22]